Understanding partial saturation in paper microfluidics enables alternative device architectures

Journal:	*Analytical Methods*
Manuscript ID	AY-ART-09-2018-001977.R1
Article Type:	Paper
Date Submitted by the Author:	27-Nov-2018

Complete List of Authors:	Buser, Joshua; University of Washington, Bioengineering Byrnes, Samantha; University of Washington, Bioengineering Anderson, Caitlin; University of Washington, Bioengineering Howell, Arielle; University of Washington, Bioengineering Kauffman, Peter; University of Washington, Bioengineering Bishop, Josh; University of Washington, Bioengineering Wheeler, Maxwell; University of Washington, Bioengineering Kumar, Sujatha; University of Washington, Bioengineering Yager, Paul; University of Washington, Department of Bioengineering

Analytical Methods

ARTICLE

Understanding partial saturation in paper microfluidics enables alternative device architectures

Received 00th January 20xx,
Accepted 00th January 20xx

DOI: 10.1039/x0xx00000x

www.rsc.org/

Joshua R. Buser*[a], Samantha A. Byrnes*[a], Caitlin E. Anderson[a], Arielle J. Howell[a], Peter C. Kauffman[a], Joshua D. Bishop[a], Maxwell H. Wheeler[a], Sujatha Kumar[a], and Paul Yager[a]

Paper-microfluidic devices are becoming more common due to their ability to automate diagnostic assays at low cost. Increasingly, paper-microfluidic devices automate more complex, multi-step assays, with the aim of bringing these assays out of the laboratory to the point-of-care. However, some common assay procedures have resisted easy automation by paper-microfluidic devices. Sample preparation procedures in particular, due to the complexity of real biological samples, still largely involve the manual execution of multiple user steps before addition to the to a paper device, often with the aid of specialized equipment. In the laboratory, most sample types are exposed to (bio)chemical treatment to release target species, which often requires additional purification steps prior to detection. Some samples, such as urine, also require concentration of target species; others, such as nasal swabs or blood, also require removal or dilution of non-target species that interfere with downstream assay steps. Additionally, the samples used in many laboratory assays require volumes (milliliter scale) too large to process efficiently with paper devices. To broaden the effectiveness and availability of point-of-care testing, we have developed and characterized a technique that automates either the concentration or dilution of large-volume samples in paper-microfluidic devices. Here we demonstrate its simplicity and broad utility in two ways: (1) an automated parallel dilution system for an immunoassay detection antibody and (2) an automated DNA extraction and concentration system for mL-sized samples. This and similar techniques rely on an improved understanding of how fluids wet porous materials and flow through multi-material networks; they confer important new capabilities to paper-microfluidic devices, the most important of which is the integration of complex sample preparation with downstream biomolecule detection.

Introduction

The use of porous materials as a platform for bioassays dates back to the 1930s with the development of paper chromatography[1–3]. In the mid to late-1970s, the home-based pregnancy test popularized the use of porous materials to bring diagnostics to the point-of-care (POC)[4–6]. More recently, George Whitesides' group helped lead a renaissance in paper-microfluidic technology when they patterned cellulose paper in two dimensions to simultaneously detect glucose and proteins in urine samples[7]. Paper-microfluidic devices have since evolved to include systems that offer advantages such as the ability to perform complex, multi-step processes[8,9], the sequential timed delivery of reagents[8,10], and compatibility with various amplification and detection techniques[11–14].

Perhaps the most useful feature of paper-microfluidic systems is passive fluid transport by capillary action. The automation of more complex assay procedures, however, has required new fluidic controls using a variety of valving techniques. For example, materials embedded into a membrane can slow or delay flow. Noh *et al*. patterned wax at various concentrations to control fluidic timing in porous devices[15,16]. Lutz *et al*. embedded sugar barriers into porous materials. Higher concentrations of sugars resulted in longer delays for fluid delivery[17]. Chen *et al*. developed a fluidic diode using a combination of hydrophobic and hydrophilic coatings to control direction and sequencing of fluid flow[18]. Many of these systems introduce an additional reagent (wax, sugar, etc.) into the reaction, which may negatively impact sensitive reactions such as nucleic acid amplification[19–21].

A number of efforts show progress in implementing valve technologies that do *not* introduce outside agents into the assay fluids. Both permanent magnets[22] and electromagnetic solenoids[23] have been used to make and break fluidic connections. These elements are outside of the main fluid pathway and do not introduce additional reagents. Toley *et al*. developed valves that use auxiliary fluidic networks to actuate expanding elements. These expanding valves can turn flow on or off and cause fluid diversion and redirection[24]. More complex switching has also been demonstrated using paper actuators, including both normally-on and normally-off single- and double-throw switches[25]. The Yager, Lutz, and Fu groups

[a] Department of Bioengineering, University of Washington, Box 355061, Seattle, WA. Email: buserj@uw.edu
*Contributed equally.
Electronic Supplementary Information (ESI) available: [details of any supplementary information available should be included here]. See DOI: 10.1039/x0xx00000x

have also designed methods for the sequential timed delivery of reagents through two-dimensional paper networks that rely on volume metering[9,26–28].

Recent publications have included reviews of additional valving for paper microfluidics including those detailed above[29–32]. Although effective, many of these systems are limited to use with a maximum of a few hundred microliters of input sample. When processing urine or dilute blood, devices may need to manage up to 5–10 mL of sample. In urine, for example, the first ~10 mL often contains the highest concentration of pathogen biomarkers[33]. Due to the dilute nature of urine, at least 1–2 mL is often collected to obtain detectable pathogen at clinically relevant concentrations[34,35].

In recent years, multiple groups have used isotachophoresis to concentrate pathogen biomarkers from complex samples [36–38], but these systems often use small sample volumes and involve multiple pre-processing steps, such as off-device centrifugation and sample dilution[39]. Additionally, isotachophoresis can be sensitive to salt and cell concentrations found in clinical samples[39]. Linnes *et al.* developed an integrated method for paper-based NA extraction coupled to in-membrane isothermal amplification to detect chlamydia[40]. Although effective, this device required multiple user steps and accepted between 10–100 µL of urine. We previously described an in-membrane sample processing method that concentrated DNA from up to 2 mL of sample, but that system did not include automation to enable development of an integrated device[41].

Alternatively, some samples require dilution prior to processing to reduce high concentrations of interfering species that may inhibit target detection[42] or restrict flow through porous membranes[41]. Previously-demonstrated paper microfluidic devices effectively dilute samples by submerging a swab in buffer, subsequently delivering the input sample into multiple detection zones causing modest dilution[43], but there are only a few demonstrations of deliberate and automated dilution in paper-based devices. Osborn *et al.* demonstrated a paper-microfluidic device capable of linear dilutions based on geometry[26] and Songjaroen *et al.* designed a system that uses a wash step to dilute a sample on-device for blood typing[44]. To date, there have not been any published reports of paper-microfluidic devices that automate multiple, parallel dilutions of a sample.

The complexity of realistic samples—some of which need concentration, and others dilution—required a re-examination of how paper-microfluidic devices process fluids, not least because the current understanding of fluid flow in these devices is based on inadequate flow models: the Washburn equation and Darcy's law. The Washburn equation is limited to one-dimensional flow, while Darcy's law can model multi-dimensional flows. However, we have recently argued that neither of these models are fully representative of complex flow in wetting porous materials because they both assume the existence of a fully saturating wetting front. In reality, a porous membrane supports a partially-saturated wetting front, where the degree of saturation depends on specific physical properties of the membrane along with fluid properties and system geometry. Therefore, we advocate the use of a flow model like the Richards equation, which is widely used in hydrogeology to model partially-saturated flow through soil[45]. Briefly, the Richards equation models the change in saturation of a porous media due to gradients in the pressure head, and can be written as:

$$\frac{\partial \theta}{\partial t} = \frac{\partial}{\partial z}\left[K(\theta)\frac{\partial H(\theta)}{dz}\right]$$

where θ is the volumetric water content, t is time, K is the hydraulic conductivity, H is the pressure head (m), and z is the position. Both the hydraulic conductivity and pressure are functions of volumetric water content: as the porous media becomes more saturated it generates less suction pressure and becomes a better fluid conductor. The full description of how to use the Richards equation as a basis for flow models for paper-microfluidic systems, and how to perform the requisite physical characterization of the composite porous materials, can be found in the PhD thesis of JR Buser, available from the University of Washington[46].

Using this new insight—that flow in paper-microfluidic devices is dependent on the existence of partially-saturated regions—we have designed a system to automate and control large-volume fluid flow in paper-microfluidic devices to support the integration of more complex sample preparation methods into these devices. We demonstrate this simple-to-use system of multiple porous materials through two examples: (1) automated DNA extraction and concentration from mL-sized samples and, to our knowledge, (2) the first demonstration of automated multiple parallel dilutions in a paper-microfluidic device.

Materials and Methods

Reagent preparation

All reagents were prepared with sterile molecular biology grade water (Fisher Scientific, Waltham, MA, USA). Low-molecular-weight chitosan oligosaccharide lactate (average MW 5000), Tris base, 2-(N-morpholino)ethanesulfonic acid (MES), achromopeptidase (ACP, A3547), ethanol, and erioglaucine were purchased from Sigma Aldrich (St. Louis, MO, USA). Glycogen was purchased from Thermo Fisher Scientific (Grand Island, NY, USA). A working solution of chitosan was prepared at 1 mg/mL in 50 mM MES at pH 5. A working solution of erioglaucine was prepared at 2 mg/mL in sterile water. A working solution of ACP was prepared at 20 U/µL in 10 mM Tris, pH 8. The 50 mM MES DNA wash buffer was prepared in sterile water and the pH was adjusted to 5. The 50 mM Tris DNA elution buffer was prepared in sterile water and the pH was adjusted to 9. All samples used in this study were from discarded human urine specimens de-identified by the Global Health STI Laboratory at the University of Washington Harborview Medical Center in Seattle, WA, USA. These samples could not be traced back to individual patients due to their discarded and de-identified nature, so a human subjects protocol was not required for this work. Urine

sample pH and salinity was measured using a pH/conductivity meter. The 40 nm InnovaCoat streptavidin–gold conjugates were purchased from InnovaBiosciences (Cambridge, United Kingdom). Triethyl ammonium bicarbonate (TEAB) at 0.1 M and biotinylated probe were supplied by ELITech Molecular Diagnostics (Seattle, WA, USA). The TEAB was diluted to 75 µM with sterile water. The biotinylated probe consisted of the following sequence: 5'–TTTTTTTTTTTTTTTTTTTT–biotinTEG–3' (T20-biotin). A working solution of T20–biotin probe was prepared at 200 µM in 75 µM TEAB. A working solution of gold nanoparticles was prepared using 40 nm, streptavidin-coated, gold nanoparticles (InnovaCoat Gold; InnovaBiosciences, Cambridge, United Kingdom) diluted to OD 0.0625 in phosphate-buffered saline buffer containing Tween-20 (0.1%, Sigma Aldrich P9416) and 1% (w/v) bovine serum albumin (PBST+BSA).

Material fabrication and patterning

All porous and plastic materials were cut to their final shapes using a CO_2 laser (VLS3.60; Universal Laser Systems, Scottsdale, AZ, USA). For DNA purification/concentration, Fusion 5 membranes (GE Healthcare Life Sciences, Niskayuna, NY, USA) were patterned with chitosan and stored in a desiccator; glass fiber (8964; Ahlstrom, Alpharetta, GA, USA) and cellulose (CFSP223000; Millipore, Billerica, MA, USA) membranes were used without modification. Test cards were made with 0.254 mm-thick Melinex backing with adhesive on one side (T-5501-10/1; Fralock, Valencia, CA, USA). For parallel dilution, nitrocellulose membranes (HF135; EMD Millipore, Billerica, MA, USA) were patterned with T20–biotin probe by a piezoelectric printer (sciFLEXARRAYER S3; Scienion AG, Berlin, Germany); 8964 glass fiber, Fusion 5, and CFSP223000 cellulose membranes were used without modification. The T20–biotin probe solution was filtered using a 0.2-µm nylon membrane (VWR, Radnor, PA, USA) at 8000g for 5 minutes prior to spotting. Test lines were created by placement of 20 spots, spaced 250 µm apart, with 30 droplets per spot. The volume of each droplet was 450–500 pL. After spotting them with T20–biotin probe solution, the nitrocellulose membranes were UV treated for 8 minutes with a UV transilluminator (UltraLUM inc, Paramount, CA, USA) at 300–310 nm and stored under desiccation before use.

Device construction

Devices were built as shown in Figure 1, Figure 3, and Figure 6, with Fusion 5 as the primary membrane and glass fiber as the secondary membrane. Cellulose was used as the waste pad for the devices in Figure 3 and Figure 6. Membranes were held in place by the adhesive layer of the Mylar test card. Device tests were run as previously described[41], with the following changes. Test samples were prepared as 10 µL of fragmented[47] MRSA gDNA (~10^4–10^5 copies/µL) diluted into 990–3990 µL of either buffer or discarded urine samples (**Table S1**) for a resulting concentration of ~10^2–10^3 copies/mL. The full sample volume was then introduced to the upstream end of the primary pathway of the device and allowed to flow through completely, followed by 250 µL of wash buffer (50 mM MES, pH 5). Then, 250 µL of the elution buffer (50 mM Tris, pH 9) was introduced to the upstream end of the secondary pathway. After the secondary pathway fully saturated, the chitosan and elution membrane sections were removed from the device. The fluid was recovered from each membrane section by centrifugation at 10,000 ×g for 3 minutes. The number of copies of target DNA in the fluid recovered from each membrane section was quantified using qPCR, then adjusted for the volume recovered from each section.

Devices were automated as shown in Figure 6. The lever arms were set to pinch closed a section of silicone tubing (STHT-C-093-2; Saint-Gobain, Valley Forge, PA, USA), which was mated to a razor-cut section of a plastic syringe (309604, BD, Franklin Lakes, NJ, USA) acting as an elution buffer reservoir. A water-soluble membrane (Water Soluble Paper, Edmund Scientific, Tonawanda, NY, USA) looped around laser-cut acrylic lever arms (8560K354, McMaster-Carr, Santa Fe Springs, CA, USA). The entire device was placed over a sample collection well to which the sample was added to initiate the test.

Device automation tests were run with test samples prepared as 10 µL of fragmented[47] MRSA gDNA (~10^4–10^5 copies) diluted into 5 mL of buffer (discarded urine samples were not used for these tests) for a resulting concentration of ~10^1–10^2 copies/mL. In these tests, however, 750 µL of elution buffer (50 mM Tris, pH 9) was loaded into the elution buffer reservoir prior to test initiation. Then, the full volume was added to the sample collection well and allowed to flow through the device without a wash step. The elution buffer automatically released upon sufficient saturation of the waste pads, which enabled sample fluid to traverse the trigger fluid delivery pathway, saturating and dissolving a break in the water-soluble paper loop. After the secondary membrane fully saturated, fluid was recovered from the elution section of the device by centrifugation at 10,000 ×g for 3 minutes. Recovery of target DNA was quantified using qPCR results and adjusting for the elution volume.

Dilution devices were built as shown in Figure 4, with glass fiber as the source pad, Fusion 5 as the sample pad, nitrocellulose as the test strip, and cellulose as the waste pad. Device tests were run by first introducing 750 µL of gold nanoparticle solution to the upstream end of the sample pad. Upon saturation of the sample pad, the glass fiber source pad was placed into a reservoir containing 3 mL of PBST, which was allowed to flow into the device until the reservoir was empty of fluid. Devices were immediately placed on a scanner (Perfection V700 Photo; Epson America, Inc., Long Beach, CA, USA) and scanned at 600 dpi in 48-bit color. The resulting images were analysed using ImageJ software (version 1.50g)[48], with which the normalized pixel intensity across the test line was quantified. A calibration curve was generated for test line intensities using known concentrations of gold nanoparticles. Dilutions of the working gold nanoparticle solution to 0–0.25 OD in PBST+BSA with a final volume of 40 µL were tested to determine the dynamic range for the system.

Total nucleic acids preparation and quantification

Nucleic acids were purified from 500 µL of discarded urine samples by first harvesting any intact cells by centrifugation at 13,000 ×g for 3 minutes. The supernatant was saved in a separate tube and cells were resuspended in an equal volume of 10 mM tris at pH 8. Cells were treated with 10 µL of 20 U/µL ACP, incubated at room temperature for 2 minutes, and then heated to 95 °C for 5 minutes.

Nucleic acids were purified from both the cell lysate and the supernatant by ethanol precipitation using 1/10 volume of 3 M sodium acetate (pH 5.2), 2 volumes of cold 100% ethanol, and 1/100 volume of 20 mg/mL glycogen. The solutions were mixed by inversion 10–12 times followed by incubation at -20 °C for 15 minutes. After incubation, the samples were centrifuged for 15 minutes at 21,000 ×g (maximum speed). The glycogen and nucleic acids formed a visible white pellet in the bottom of the tube. The supernatant was removed and the pellet was washed with 1 mL of 70% ethanol. The sample was mixed by inversion 10–12 times followed by centrifugation at maximum speed for 5 minutes. The supernatant was removed and the pellet air-dried for 10 minutes at room temperature. The pellet was then resuspended in 50 µL of sterile water and incubated at 37 °C for 10 minutes. The resulting concentration of nucleic acids was quantified using a Nanodrop (ThermoFisher Scientific, Grand Island, NY, USA).

MRSA ldh-1 gene quantification

DNA recovery was quantified using a qPCR kit for the *ldh*-1 gene provided by the ELITechGroup (ELITechGroup Molecular Diagnostics, Bothell, WA, USA). The 20 µL reactions were run on a real-time PCR instrument (CFX96; Bio-Rad, Hercules, CA, USA) using the following protocol: 50 °C hold for 2 minutes; 93 °C hold for 2 minutes; 45 cycles of 93 °C for 10 seconds, 56 °C for 30 seconds, and 72 °C for 15 seconds; and 72 °C hold for 5 minutes. Fluorescence data were collected in the Texas Red channel during the 56 °C step of each cycle. The qPCR results were analysed using the automated threshold cycle (CT) value calculation in the CFX Manager software (Bio-Rad, Hercules, CA, USA). This assay is sensitive down to ~10^1 copies of the target sequence.

Statistics

All statistics were run using the open-source statistical package R (64 bit, version 3.0.2)[49].

Results and Discussion

Control of large-volume fluid flow in paper-microfluidic systems using partial saturation

Porous materials enable affordable diagnostic devices (e.g. lateral flow tests) in part because they automatically transport fluids, removing the need for expensive operational equipment such as syringe pumps. In general, paper-microfluidic systems are complex, multi-material porous networks in which fluid transport is driven by material properties, and by saturation and pressure differentials at the junction of overlapping materials. However, previous descriptions of fluid transport in paper-microfluidic systems assume a single-material, single-dimensional system, and a fully saturating wetting front.

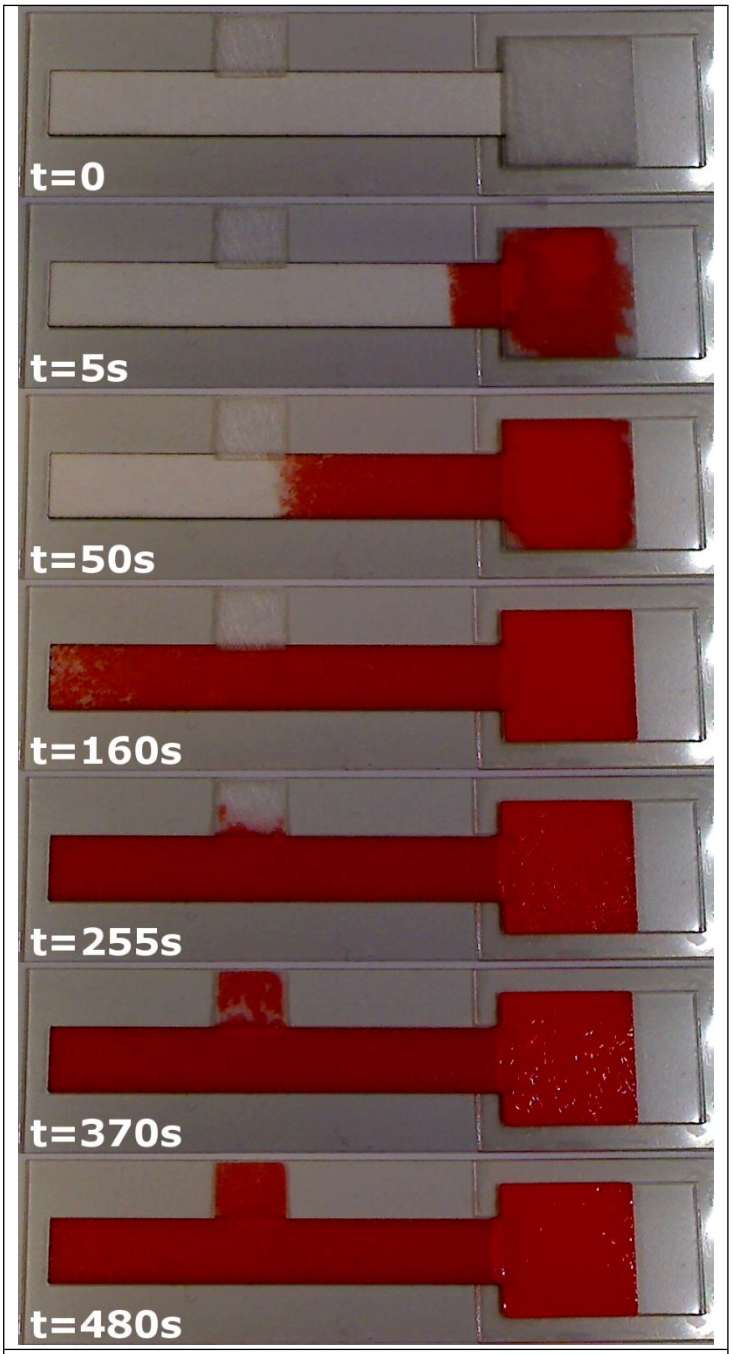

Figure 1: Using partial saturation to control flow in a paper microfluidic system. A red dye solution is added to the square glass fiber source pad, which drains into a strip of Fusion 5 membrane, referred to as the "primary membrane". An additional section of glass fiber membrane is positioned partially down the Fusion 5 strip, referred to as the "secondary membrane". This glass fiber section will remain largely dry until the fluid has completely wet the length of Fusion 5 membrane.

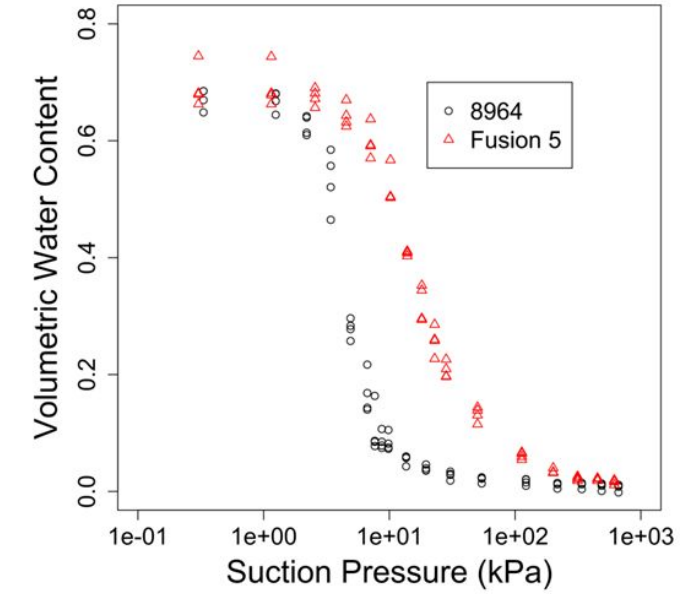

Figure 2: Water retention curves for 8964 glass fiber and Fusion 5 membrane illustrate the fluid pressure at varied levels of membrane saturation. Fusion 5 generates a higher suction pressure than 8964 for a given volumetric water content.

The assumption that the wetting front in paper-microfluidic systems is fully saturating is particularly problematic, as even simple paper-microfluidic demonstrations will show (see Figure 1). However, more advanced paper-microfluidic systems become possible when partial saturation is exploited during the design process. The system of Figure 1 is an example, where a glass fiber section positioned part-way down a length of Fusion 5 membrane will stay dry until the Fusion 5 membrane has become fully saturated. However, the system cannot be modelled with the Washburn equation, because it is composed of multiple membrane types with distinct fluid transport properties. The system should not be modelled with Darcy's law, as Darcy's law would incorrectly predict that the fully saturated wetting front would move into the glass fiber section as soon as the dye solution reached it. Fortunately, the system can be modelled with the Richards equation, which was originally developed to describe partially saturated fluid transport in hydrogeological systems.

To model this system with the Richards equation, some material properties must be known. Methods developed for quantifying these properties, in the form of water retention curves[50], can be adapted to paper-microfluidic systems. We have generated water retention curves for Fusion 5 and a glass fiber material, for example, shown in Figure 2, using just a lab centrifuge and modified filter spin columns.

The water retention curves plotted in Figure 2 show that Fusion 5 generates a larger suction pressure than 8964 at any equivalent volumetric water content. Therefore, in a fluid-limited system that uses both materials, such as that of Figure 1, the Fusion 5 will have a larger volumetric water content because of its greater suction pressure. However, once the wetting front reaches the end of the Fusion 5 membrane its suction pressure will drop as the membrane continues to saturate. Eventually the suction pressure will fall below that of the 8964 glass fiber, at which point the 8964 glass fiber will fill with fluid starting at the junction. Careful material selection allows predictable pressure differentials at material junctions and, therefore, controllable material wetting and fluid flow.

Figure 3A shows a paper-microfluidic system constructed in a similar fashion. Fusion 5 is connected to a fluid source and a waste pad in a primary fluidic pathway, and is sandwiched between two pieces of 8964 glass fiber that make up a secondary fluidic pathway, creating an overlap region between the primary and secondary pathways, Figure 3B. During wetting, the primary pathway will take up fluid, Figure 3C. The secondary pathway remains dry as the fluid flows through the overlap region. When an additional fluid source is connected to the secondary pathway, the fluid flows through and across the overlap region. We have found the simple switching behavior provided by this system to be useful in a variety of paper-microfluidic contexts. Next, we show applications of the system with particular relevance to two common sample preparation steps: dilution and concentration.

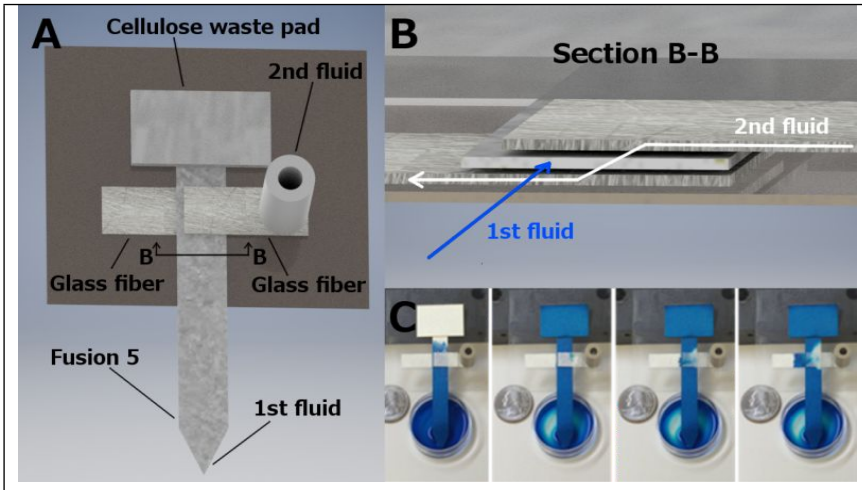

Figure 3: Using partial saturation for flow control in a paper microfluidic device. A. Overview. The 1st fluid flows through Fusion 5 and into a cellulose waste pad without wetting the overlapping glass fiber sections. When the 2nd fluid is added, flow is redirected in a perpendicular direction through the junction. B. Cross section of overlapping region. The 1st fluid flows past the glass fiber without wetting it, the 2nd fluid, when added, flows through the junction from right to left. C. Images showing device operation with a blue dye solution as the 1st fluid and water as the 2nd fluid.

integrated. This prototype device was designed to create a

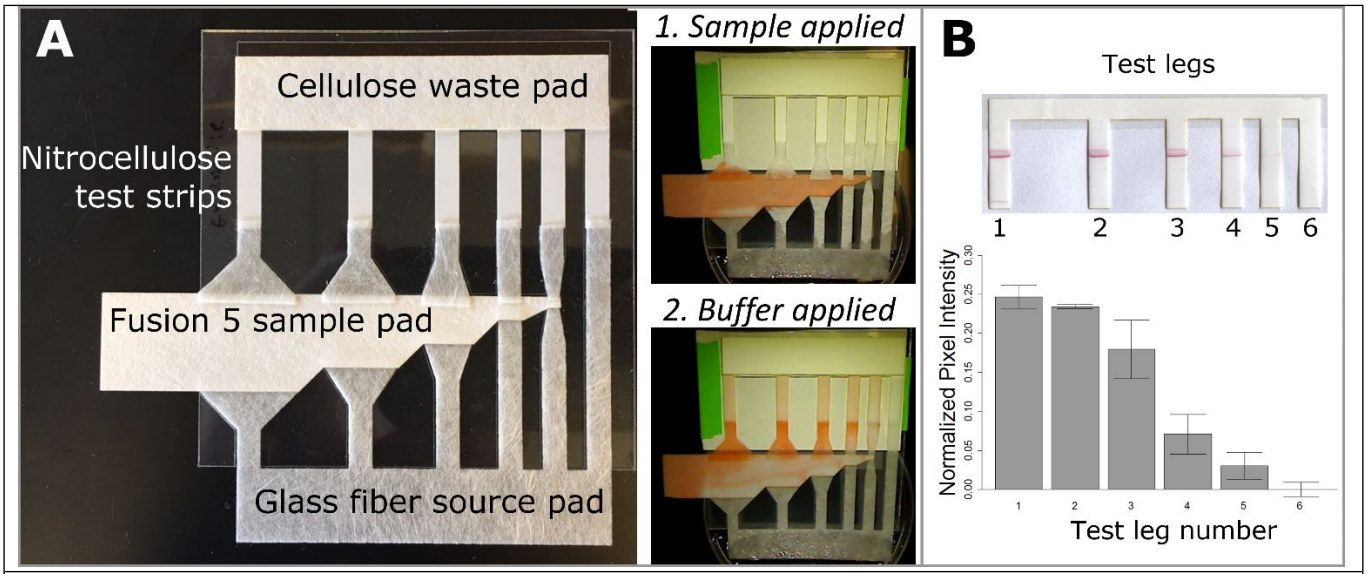

Figure 4: Paper-microfluidic device for automated dilution. A. Device schematic of the automation dilution device, where sample first flows through the Fusion 5 sample pad, followed by applying running buffer to the source pad. Video stills of the dilution device using red dye are shown. B. Representative test lines and the calculated normalized pixel intensity for each leg of the automated diluter. Averages of N=3 are reported with error bars representing +/- one standard deviation.

Multiple, parallel dilutions of samples using partial saturation for flow control

Controlled dilution is a commonly-used laboratory technique in chemistry, biochemistry and biology. Diagnostic applications using a dilution series range from measuring binding kinetics to performing sample preparation[51,52]. For an example of the latter, some samples require dilution to reduce high concentrations of species that inhibit target detection. While plastic-microfluidic devices have been used to generate dilution series, they require additional equipment to pump fluids through the device[51–53]. Paper-microfluidic devices automate fluid transport but have not yet been shown to combine automated sample dilution with molecular detection. Such a combination would enable paper-microfluidic devices to scale up small sample volumes and samples that contain high concentrations of assay inhibitors.

Therefore, we prototyped a paper-microfluidic device, shown in Figure 4A, that uses a series of "partial saturation switches" to automate the creation and delivery of a dilution series from a sample and to multiple test strips, respectively. To operate the device, the sample was applied to a sample pad, which formed the primary pathway of the switch. The source pad was then placed into buffer, which hydrated the secondary pathway and carried the series of sample dilutions into the test strips.

We found the area of overlap between the primary and secondary pathways to be related to the dilution factor on the sample carried into the secondary pathway. By simple changes in geometry, an arbitrary dilution series can be created with this system that delivers various, specific amounts of a sample, or reagent, across a number of test lines. Both linear and logarithmic series are among those possible to create, depending on the biochemical or biological assay being linear dilution series.

The dilution factors were quantified using nitrocellulose test strips, with capture lines comprising UV-cross-linked, biotin–oligonucleotide conjugates. The sample was spiked with streptavidin–gold nanoparticle conjugates, which were bound by the immobilized biotin–oligo conjugates on the capture line, Figure 4B. We generated a calibration curve (Figure S1) by quantifying test strip pixel intensity using known concentrations of gold nanoparticles. Based this data, the dilutions achieve range from 80% of the original concentration down to 10% of the original concentration. The dilution achieved is linearly related to the Fusion 5 sample pad area for each respective leg (data not shown, $R^2 = 0.96$).

We anticipate that an automated dilution series can be integrated into a variety of devices to support more complex sample preparation techniques and multi-step assays. In particular, the use of an automated dilution series can enable quantitative readout for nucleic acid amplification or conventional lateral flow immunoassay applications, which traditionally limited to non-quantitative or semi-quantitative results.

Concentration of target DNA from mL-sized samples using partial saturation for flow control

In this automated, paper-microfluidic switching system fluid initially flows through one pathway in the network. A secondary elution flow is later redirected through a second pathway. This is used to extract and concentrate DNA from 1 mL samples when combined with a previously demonstrated system for DNA capture and release [41]. The capture-and-release system used membrane-patterned chitosan, which is a linear polysaccharide that electrostatically captures DNA when the pH is below ~6.3–6.5, the pKa of the primary amine [54,55]. Above that pH, the amines are deprotonated and the electrostatic interaction is released. In this work, we

constructed a simple device that combined these systems, and measured its ability to recover target DNA spiked into 1 mL samples of discarded human urine from hospital patients, as shown in Figure 5. Recovery of target DNA from urine samples using this device was >80%, but recovery efficiency appears to be correlated with the pH of the sample itself.

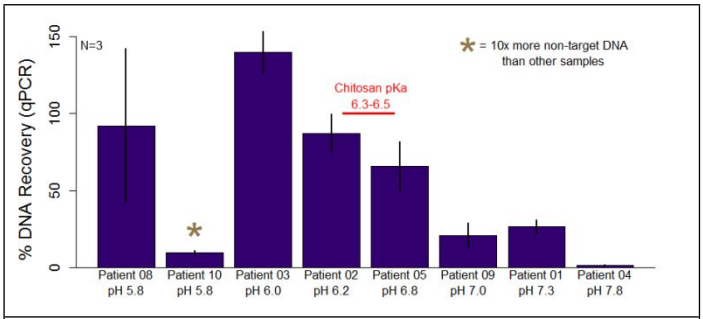

Figure 5: In-membrane DNA purification and concentrated from 1 mL urine samples using a system similar to Figure 3. The primary membrane (Fusion 5) was patterned with a DNA-capture polymer. Flow of the 1 mL urine sample through primary the membrane resulted in DNA captured by the polymer in the at the membrane junction. After a wash step through the primary membrane, an elution buffer was introduced to the secondary membrane (8964 glass fiber) causing the DNA to flow through the junction and into the elution region. Sample recovery was quantified with qPCR. Averages of N=3 are reported with error bars representing +/- one standard deviation. Generally, as sample pH increased, recovery of target DNA decreased with the exception of Patient 10. The non-target DNA in this sample likely overwhelmed the capacity of the DNA purification system leading to poor recovery of target DNA.

Unsurprisingly, most of the samples with pH values at or below 6.8 (samples 02, 03, 05, and 08) showed high recovery of target DNA, while all of samples with pH values higher than 7 (samples 01, 04, and 09) show reduced recovery. The exception was sample 10 which had an appropriate pH for DNA capture by chitosan, but showed very low DNA recovery. We hypothesize that sample 10 had reduced recovery due to an overloading of the chitosan with non-target nucleic acids that were introduced by the patient sample itself (patient 10 had 10x more non-target nucleic acids compared to the rest of the samples tested). Based on previous work, this amount of non-target nucleic acid is above the capacity of the chitosan patterned in this membrane. Sample 8 also had highly variable recovery, even though the average was high and followed the expected pattern based on sample pH. This variation was potentially due to the high salinity of sample 8. High salt content may shield the electrostatic interaction between chitosan and nucleic acids, causing inconsistent recovery[56,57]. Table S1 shows our detailed characterization of each of the patient samples.

The amount of DNA remaining in the chitosan region after elution was less than 10% of the input for each sample. The device runtimes were 13-15 minutes. The geometry of the materials in this device was optimized to decrease runtime, particularly that of the waste pads. Material choice is also important, but stacking waste pads reduced runtime because it increased the volumetric fluid uptake and minimized the fluid transport distance. In fact, using a stack of multiple, small waste pads instead of a single, large waste pad significantly reduced the device runtime (Figure S2).

These results were promising, but still required one user step to add the sample and a second, timed user step to add an elution buffer. We therefore constructed a more automated device that integrated the release of the elution buffer at the appropriate time.

Automated processing of samples using partial saturation to actuate a mechanical valve

We added an automatic release mechanism to the device to deliver the elution buffer after the cellulose waste pad sufficiently saturated with sample, Figure 6. The mechanism operated as follows. First, the sufficiently saturated waste pad caused the dissolution of a connected loop of water-soluble membrane, which held a mechanical valve in a closed position. The automatic release of the mechanical valve upon dissolution of the loop, described in more detail below, allowed the elution buffer to flow into the secondary pathway. Importantly, this mechanism gave us control over the volume of processed sample that caused the release of the elution buffer. We controlled that relationship through careful design of the waste pad geometry and the water-soluble loop location.

The mechanical valve comprised a section of silicone tubing and a surrounding pair of lever arms. The valve was closed when the loop of water-soluble membrane held the lever arms together, which compressed the silicone tubing into a watertight seal, Figure 6B. The valve was opened when the loop dissolved and freed the lever arms to separate, which allowed the silicone tubing to open and pass elution buffer through to the secondary pathway from a reservoir above, Figure 6C.

Still images from a video of a flow test using green and yellow dyes in water demonstrated the basic operation of the automated device (Figure 6D). Dye tests were used to evaluate various optimizations of the automated device with respect to fluidic performance. The waste pad geometry and water-soluble loop connection were optimized to automatically process a 1 mL sample volume. The overlap between the primary and secondary fluid pathways was optimized to maximize DNA elution.

We found in early iterations of the automated device that a single flow path at the overlap led to loss of eluted DNA to upstream and downstream portions of the primary pathway (due to partial saturation of the primary pathway). Therefore, we tested two- and three-leg versions of the secondary pathway, which saturated the upstream and/or downstream portions of the primary pathway with elution buffer. The three-leg geometry yielded the best fluidic performance in dye tests, Figure S3A, as it effectively stopped flow upstream and downstream in the primary pathway, which should cause eluted DNA to flow only into the downstream elution region of the secondary pathway. We therefore used the three-leg design in all subsequent design iterations.

We also optimized the amount of overlap between the primary and secondary pathways to improve DNA elution. Dye tests showed that larger overlap areas led to a more complete wash out of the overlap region, Figure S3B, which should improve both recovery percentage and concentration factor of

the DNA. To confirm, we followed the dye tests with device tests using DNA spiked into 1 mL of capture buffer. These results were that the "top full, bottom partial" geometry resulted in the highest recovery of DNA, with the lowest standard deviation, Figure S3C, and concentration factor, Figure S2C. We therefore used this geometry in all subsequent design iterations.

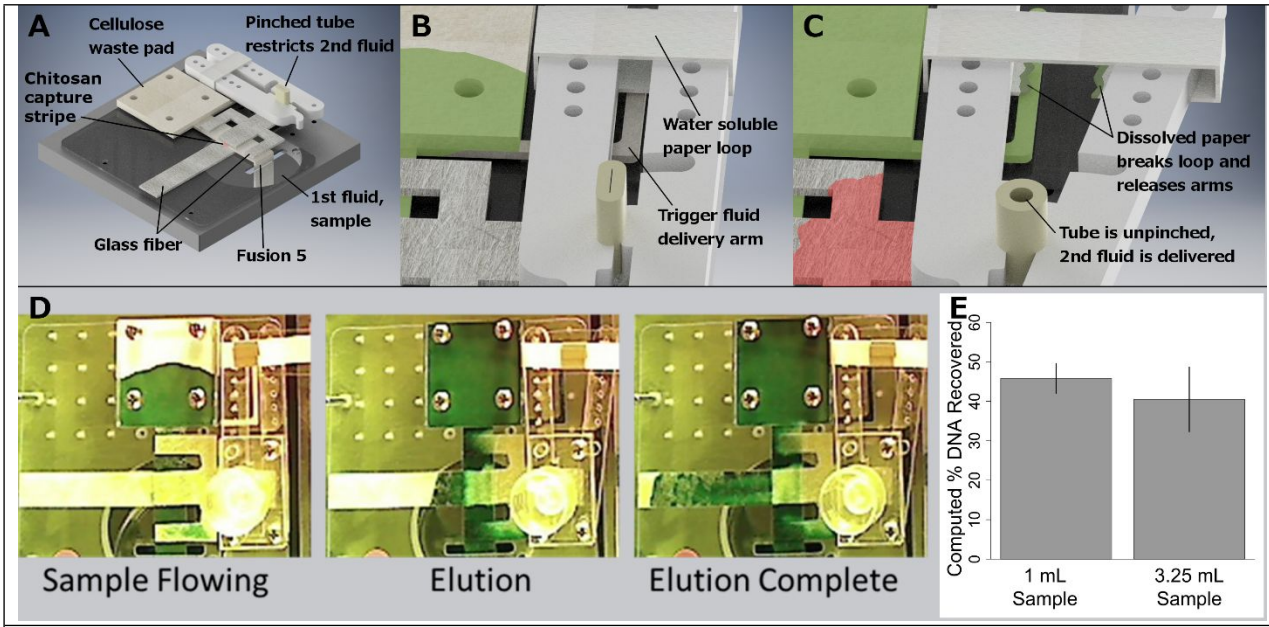

Figure 6: Device automation for large volume sample DNA concentration. A: Initially, the 1st fluid (sample) flows via fusion 5 through the capture zone and into the waste pad. The glass fiber sections do not wet until the 2nd fluid (elution buffer) is released. B: The second fluid is restricted with pinched tubing. When the sample fluid wets the water soluble paper loop, part of the loop will dissolve. C: When the loop breaks, the pinched tubing is released, delivering fluid from the 2nd fluid (elution buffer) reservoir (not shown). D: Visualization of device operation. A blue dye solution is substituted for the sample, and water for the elution buffer. The elution buffer release is triggered by the saturation of the cellulose wicking pad. E: DNA purification and concentration experiment using the automated device. Averages of N=6 are reported with error bars representing +/- standard error. The 1 mL samples were processed in 12–13 minutes while the 3.25 mL samples were processed in 32–33 minutes.

The final device design was tested with 1 and 4 mL sample volumes (the devices, optimized for 1 mL samples, only processed 3.25 mL of the 4 mL before the valve released), with all samples spiked with purified DNA. Multiple elution fractions (~60 µL each) were collected from each device, Figure S4. Overall, the fully automated device recovered ~40 % of the DNA, Figure 6E. In addition, the fractions provided a discrete view of DNA elution from the capture region over time, which corresponded to a discrete spatial distribution of eluted DNA. The majority of the DNA was recovered in the first two elution fractions, Figure S4, which indicated effective concentration into a volume (120 µL or less) reasonably compatible with most biochemical assays (e.g. nucleic acid amplification). We quantified the concentration effect using qPCR. For the 1 and 3.25 mL samples, the concentration factors ranged from 1.8–2.9 and 5.2–8.3, respectively (Equation S1). The method we've presented here results in similar recovery of DNA from spiked samples compared to common, gold standard purification methods[58,59]. Additionally, this system is less time-consuming than a multi-step Qiagen kit or ethanol precipitation protocol.

DNA purification and concentration traditionally relies on methodologies employing significant equipment and disposable labware. A fully integrated device of this type would provide highly sensitive diagnostic information in an automated sample-to-result manner, from a range of sample types, on an inexpensive paper-microfluidic system, and in a

Conclusions

Here we have shown two example applications utilizing the partially-saturated nature of capillary-driven flow in paper microfluidics, enabling capture of DNA from mL-sized clinical urine samples, and providing a dilution series of a sample. These approaches rely on the same inexpensive materials as other paper microfluidic devices, and enable enhanced functionality by harnessing the complexity of flow in these systems. An improved understanding of partially-saturated flow enables new architectures using composite networks of porous media specially chosen by their respective wetting properties.

Conflicts of interest

There are no conflicts to declare.

Acknowledgements

This work was supported by a grant to Paul Yager from the Defense Advanced Research Projects Agency (DARPA) "Multiplexable Autonomous Disposable for Nucleic Acid Amplification Tests for LRSs" under Grant No. HR0011-11-2-0007. We thank our colleagues Ryan Gallagher, Dr. Paula Ladd, and Dr. Erin Heiniger in the Yager Laboratory who provided

valuable discussion and feedback on experimental design and analysis. We thank all of our colleagues in the Harborview STI Clinic who provided discarded, de-identified samples and valuable discussion and feedback on experimental design and analysis. We also thank our collaborators from ELITechGroup Molecular Diagnostics for supplying reagents for the qPCR assay and lateral flow detection reagents.

References

1 H. Yagoda, *Ind. Eng. Chem. - Anal. Ed.*, 1937, **9**, 79.
2 R. H. Muller and D. L. Clegg, *Anal. Chem.*, 1949, **21**, 1123.
3 R. Consden, A. H. Gordon and A. J. P. Martin, *Biochem. J.*, 1944, **38**, 224.
4 U. K. Banik, M. A. Hirsch, D. S. Irvine, J. Krupey, A. Hurwitz, K. Singh, J. Wetsel and M. L. Givner, *Fertil. Steril.*, 1979, **32**, 426.
5 EPT Do-It-Yourself Early-Pregnancy Test. *Med. Lett. Drugs Ther.*, 1978, **20**, 39.
6 S. Arora and S. Tyagl, *Clinician (Goa).*, 1978, **42**, 179.
7 A. W. Martinez, S. T. Phillips, M. J. Butte and G. M. Whitesides, *Angew. Chem. Int. Ed. Engl.*, 2007, **46**, 1318.
8 E. Fu, B. Lutz, P. Kauffman and P. Yager, *Lab Chip*, 2010, **10**, 918.
9 B. R. Lutz, P. Trinh, C. Ball, E. Fu and P. Yager, *Lab Chip*, 2011, **11**, 4274.
10 G. E. Fridley, H. Q. Le, E. Fu and P. Yager, *Lab Chip*, 2012, **12**, 4321.
11 E. Fu, P. Kauffman, B. Lutz and P. Yager, *Sens. Actuators. B. Chem.*, 2010, **149**, 325.
12 N. M. Rodriguez, J. C. Linnes, A. Fan, C. K. Ellenson, N. R. Pollock and C. M. Klapperich, *Anal. Chem.*, 2015, **87**, 7872.
13 B. Rohrman and R. Richards-Kortum, *Anal. Chem.*, 2015, **87**, 1963.
14 B. A. Rohrman and R. R. Richards-Kortum, *Lab Chip*, 2012, **12**, 3082.
15 H. Noh and S. T. Phillips, *Anal. Chem.*, 2010, **82**, 8071.
16 H. Noh and S. T. Phillips, *Anal. Chem.*, 2010, **82**, 4181.
17 B. Lutz, T. Liang, E. Fu, S. Ramachandran, P. Kauffman and P. Yager, *Lab Chip*, 2013, **13**, 2840.
18 H. Chen, J. Cogswell, C. Anagnostopoulos and M. Faghri, *Lab Chip*, 2012, **12**, 2909.
19 S. F. An and K. A. Fleming, *J. Clin. Pathol.*, 1991, **44**, 924.
20 W. A. Al-soud and P. Rådström, *J. Clin. Microbiol.*, 2001, **39**, 485.
21 C. Schrader, A. Schielke, L. Ellerbroek and R. Johne, *J. Appl. Microbiol.*, 2012, **113**, 1014.
22 M. Fratzl, B. S. Chang, S. Oyola-Reynoso, G. Blaire, S. Delshadi, T. Devillers, T. Ward, N. M. Dempsey, J.-F. Bloch and M. M. Thuo, *ACS Omega*, 2018, **3**, 2049.
23 T. H. Kim, Y. K. Hahn, J. Lee, D. Van Noort and M. S. Kim, *Anal. Chem.*, 2018, **90**, 2534.
24 B. J. Toley, J. A. Wang, M. Gupta, J. R. Buser, L. K. Lafleur, B. R. Lutz, E. Fu and P. Yager, *Lab Chip*, 2015, **15**, 1432.
25 T. Kong, S. Flanigan, M. Weinstein, U. Kalwa, C. Legner and S. Pandey, *Lab Chip*, 2017, **17**, 3621.
26 J. L. Osborn, B. Lutz, E. Fu, P. Kauffman, D. Y. Stevens and P. Yager, *Lab Chip*, 2010, **10**, 2659.
27 P. Kauffman, E. Fu, B. Lutz and P. Yager, *Lab Chip*, 2010, **10**, 2614.
28 S. Dharmaraja, L. Lafleur, S. Byrnes, P. Kauffman, J. Buser, B. Toley, E. Fu, P. Yager and B. Lutz, 2013, **8615**, 86150X.
29 B. Srinivasan and S. Tung, *J. Lab. Autom.*, 2015, **20**, 365.
30 S. Ahmed, M. P. N. Bui and A. Abbas, *Biosens. Bioelectron.*, 2016, **77**, 249.
31 Y. He, Y. Wu, J. Z. Fu and W. B. Wu, *Rsc Adv.*, 2015, **5**, 78109.
32 S.-G. Jeong, J. Kim, S. H. Jin, K.-S. Park and C.-S. Lee, *Korean J. Chem. Eng.*, 2016, **33**, 2761.
33 M. Chernesky, D. Jang, S. Chong, J. Sellors and J. Mahony, *Sex. Transm. Dis.*, 2003, **30**, 345.
34 C. A. Wisniewski, J. A. White, C.-E. C. Michel, L. Mahilum-Tapay, J. P. V Magbanua, E. C. B. Nadala, P. J. Barber, B. T. Goh and H. H. Lee, *J. Clin. Microbiol.*, 2008, **46**, 1466.
35 S. F. Isbey, T. M. Alcom, R. H. Davis, J. Haizlip and P. A. Leone, *Genitourin. Med.*, 1997, **73**, 378.
36 A. Rogacs, L. a. Marshall and J. G. Santiago, *J. Chromatogr. A*, 2014, **1335**, 105.
37 M. D. Borysiak, K. W. Kimura and J. D. Posner, *Lab Chip*, 2015, **15**, 1697.
38 B. Y. Moghadam, K. T. Connelly and J. D. Posner, *Anal. Chem.*, 2014, **86**, 5829.
39 M. Bercovici, G. V Kaigala, J. C. Liao and J. G. Santiago, *14th Int. Conf. Miniaturized Syst. Chem. Life Sci. 2010, MicroTAS 2010*, 2010, **2**, 797.
40 J. C. Linnes, A. Fan, N. M. Rodriguez, B. Lemieux, H. Kong and C. M. Klapperich, *RSC Adv.*, 2014, **4**, 42245.
41 S. A. Byrnes, J. D. Bishop, L. Lafleur, J. R. Buser, B. Lutz and P. Yager, *Lab Chip*, 2015, **15**, 2647.
42 J. Noiphung, K. Talalak, I. Hongwarittorrn, N. Pupinyo, P. Thirabowonkitphithan and W. Laiwattanapaisal, *Biosens. Bioelectron.*, 2015, **67**, 485.
43 L. K. Lafleur, J. D. Bishop, E. K. Heiniger, R. P. Gallagher, M. D. Wheeler, P. C. Kauffman, X. Zhang, E. C. Kline, J. R. Buser, S. Kumar, S. A. Byrnes, N. M. J. Vermeulen, N. K. Scarr, Y. Belousov, W. Mahoney, B. J. Toley, P. D. Ladd, B. R. Lutz, P. Yager, S. Ramachandran, S. A. Byrnes, N. M. J. Vermeulen, N. K. Scarr, Y. Belousov, W. Mahoney, B. J. Toley, P. D. Ladd, B. R. Lutz, P. Yager, S. Kumar, S. A. Byrnes, N. M. J. Vermeulen, N. K. Scarr, Y. Belousov, W. Mahoney, B. J. Toley, P. D. Ladd, B. R. Lutz and P. Yager, *Lab Chip*, 2016, **16**, 3377.
44 T. Songjaroen and W. Laiwattanapaisal, *Anal. Chim. Acta*, 2016, **921**, 67.
45 L. A. Richards, *Physics*, 1931, **1**, 318.
46 J. R. Buser, PhD Thesis, University of Washington, 2016.
47 S. A. Byrnes, J. D. Bishop and P. Yager, *Anal. Methods*, 2017, **9**, 3450.
48 C. A. Schneider, W. S. Rasband and K. W. Eliceiri, *Nat. Methods*, 2012, **9**, 671.
49 R: A Language and Environment for Statistical Computing, R Core Team, R Foundation for Statistical Computing Vienna, Austria, 2018. https://www.R-project.org.
50 ASTM D6836 − 02 , *Standard Test Methods for*

Determination of the Soil Water Characteristic Curve for Desorption Using Hanging Column , Pressure Extractor , Chilled Mirror Hygrometer , or Centrifuge 1, 2015, vol. 02.

51 B. M. Paegel, W. H. Grover, A. M. Skelley, R. A. Mathies and G. F. Joyce, *Anal. Chem.*, 2006, **78**, 7522.

52 J. Nguyen, Y. Wei, Y. Zheng, C. Wang and Y. Sun, *Lab Chip*, 2015, **15**, 1533.

53 C. Kim, K. Lee, J. H. Kim, K. S. Shin, K.-J. Lee, T. S. Kim and J. Y. Kang, *Lab Chip*, 2008, **8**, 473.

54 S. Danielsen, K. M. Vårum and B. T. Stokke, *Biomacromolecules*, 2004, **5**, 928.

55 G. Maurstad, S. Danielsen and B. T. Stokke, *Biomacromolecules*, 2007, **8**, 1124.

56 P. Debye, *Phys. Zeitschrift*, 1923, **24**, 185.

57 M. Ullner and D. Langevin, in *DNA Interactions with Polymers and Surfactants*, eds. R. Dias and B. Lindman, John Wiley & Sons, Inc., Hoboken, New Jersey, 2008, pp. 9–10, 266–267.

58 R. Boom, C. J. Sol, M. M. Salimans, C. L. Jansen, P. M. Wertheim-van Dillen and J. van der Noordaa, *J. Clin. Microbiol.*, 1990, **28**, 495.

59 P. Chomczynski, *Anal. Biochem.*, 1987, **159**, 156.